ELSEVIER

Chemical Engineering Journal 72 (1999) 185–193

Chemical Engineering Journal

Study of mass transfer in a novel gas–liquid contactor: the aero-ejector

G.M. de Billerbeck[a], J.S. Condoret[b], C. Fonade[a,*]

[a]*Institut National des Sciences Appliquées, Centre de Bioingénierie G. Durand (CNRS UMR 5504, L.A. INRA) Complexe Scientifique de Rangueil, 31077, Toulouse Cedex 4, France*

[b]*Ecole Nationale Supérieure d'Ingénieurs de Génie Chimique (CNRS UMR 5503), Chemin de la Loge, 31077, Toulouse, France*

Received 22 April 1998; received in revised form 27 July 1998; accepted 4 September 1998

Abstract

This work has given the first insight into the mass transfer performances of a new contacting apparatus, the aero-ejector, which allows the processing of high gas-to-liquid ratios in a small sized device. Conventional liquid-side controlled oxygen transfer was tested which allows the quantitative comparison of this technology with existing technology. We have also demonstrated the ability of this device to solve an actual engineering problem, that is, the elimination of VOCs, assimilated here to ethanol. © 1999 Elsevier Science S.A. All rights reserved.

Keywords: Mass transfer; Gas–liquid contactor; VOCs absorption; Aero-ejector

1. Introduction

This work deals with the treatment of industrial gaseous wastes which concerns many industries: automobile industry, petrochemical, printing, fine and heavy chemicals industry, etc. Among the different gaseous wastes, the purification of those containing volatile organic compounds (VOCs) presents special difficulties because of the large gas volumes to be treated and of the low concentrations of pollutants.

Conventional VOC elimination techniques are essentially of three types: adsorption, combustion and biological degradation. Adsorption techniques are useful when the recuperation of VOCs is economically worthwhile. This is particularly the case when the effluent mainly contains one VOC. Combustion techniques are also applicable when the VOC concentration is sufficiently high to maintain combustion. The principle of biotechnological processes is to use a gas–liquid contactor to transfer VOCs from the gas phase to the liquid phase, where they are degraded by specific microorganisms. They are particularly suited to the purification of gaseous effluents containing dilute VOCs.

In fact, the gas–liquid contactor has the important and difficult duty of transferring VOCs from large gas volumes at dilute concentration to small liquid volumes. This implies the use of non-conventional gas–liquid contacting devices.

Since 1986, our laboratory has been studying a new gas–liquid contactor, the hydro-ejector. The incentive for its application in biotechnological processes for gaseous waste treatment is its capacity to create a highly turbulent two-phase flow. Good mass transfer can thus be achieved under the energetic and size conditions compatible with industrial constraints. This new technology will first be briefly presented after a survey of the existing technology.

The mass transfer rate is directly related to the gas–liquid interfacial area and to the value of the mass transfer coefficient. These two parameters are a consequence of the specific power used to run the contactor. The different gas–liquid contacting devices are distinguished by the way they degrade this energy to achieve the contact and the mass transfer between the gaseous and liquid phases. They are usually classified into the following categories.

1.1. Dispersed gas contactors

Mechanically agitated contactors, bubble columns and plate columns are efficient gas–liquid contactors when the gas and liquid volumes brought into contact lead to a bubble dispersion. Moreover, when mass transfer is accompanied by chemical reaction, these contactors are suited to slow reactions developing mainly in the bulk of the liquid. These contactors are, therefore, not particularly suited to VOC

*Corresponding author.

1385-8947/99/$ – see front matter © 1999 Elsevier Science S.A. All rights reserved.
PII: S1385-8947(98)00132-6

elimination because of the large gas-to-liquid ratios associated with this application.

1.2. Dispersed liquid contactors

Spray columns, wetted wall columns, packed columns and Venturi contactors are dispersed liquid gas–liquid contactors. These contactors are suited to contact operations where the gas-to-liquid ratio is high. When mass transfer in these contactors is accompanied by chemical reaction, they work particularly well in the case of instantaneous or rapid reactions in the liquid film next to the interface. This type of contactor could be associated with a bioreactor for the biological treatment of gaseous effluents containing VOCs. However, the first three quoted contactors are particularly bulky because of the low superficial gas velocity they require. In contrast, Venturi type contactors are suited to operations with large gas-to-liquid volume ratios. Moreover, they can satisfy the low gas pressure drop constraint imposed by the industrial use of rotary blowers or fans for the gas compression.

1.3. Venturi type contactors

There are two types of Venturi contactors: those whose geometry is that of a conventional Venturi and those composed of an ejector with a convergent and a divergent section. The latter type is called a hydro-ejector or simply an ejector. Ejectors are generally liquid driven but both types of Venturi contactors can be liquid or gas driven. They are usually associated with a downstream phase separation system. Although some mass transfer takes place in the separation system, it is essentially performed inside the Venturi contactor.

In liquid driven Venturi devices (Venturi ejectors, tubular ejectors, hydro-ejectors), the gas is naturally dragged along by the liquid flow. The two-phase flow obtained contains the liquid as the continuous phase and the dispersed gas as bubbles. The gas–liquid flow ratio, defined as the ratio of the gas to the liquid volumetric flow, is then relatively small, 0.3, for conventional Venturi contactors [1] and up to 4 for hydro-ejectors. Liquid driven Venturi devices have been studied by Touré [2], Bouhelassa and Zoulalian [3,4], Briens et al. [5], Hadjidakis [6], Belhaj et al. [7], Melbourne and Jackson [8], Bauer et al. [9] (conventional Venturis), and Rainer et al. [10] (hydro-ejectors). The gas–liquid flow ratio does not correspond to our field of application, where $Q_G/Q_L \cong 30$ to 40.

In gas driven Venturi contactors, the gas–liquid flow ratio can be very high (up to 1000). In this case, the gas is the continuous phase and the liquid is dispersed into tiny drops. Gas driven Venturi contactors are used for gas–liquid mass transfer [6,11–14] and for dust elimination in gaseous effluents [15–17]. In this work, we consider a new gas–liquid contactor, the aero-ejector, which could be classified as a gas driven Venturi, although its internal geometry is substantially different. We aim to estimate volumetric film mass transfer coefficients from absorption of oxygen and of a model VOC, i.e., ethanol.

2. Principle of the aero-ejector

The gas–liquid contacting system studied here is composed of the aero-ejector itself followed by a phase separation column. Several aero-ejectors can be associated with the same separation column to treat larger gas flow rates.

The aim of the aero-ejector is to generate intimate contact between the gas effluent and the absorbing liquid, which will afterwards be purified in a bioreactor. Its internal geometry is derived from the hydro-ejector proposed by Fonade and developed by Rainer et al. [10] for oxygenation in biological processes.

The hydro-ejector is a liquid driven device and the gas-to-liquid flow rate ratio obtained is in the range of 4 to 5. The high turbulence generated inside the hydro-ejector intensifies the gas–liquid mass transfer: using deoxygenated water and ambient air, Rainer et al. [10] showed that the dissolved oxygen concentration in the liquid phase of the two-phase jet generated by the hydro-ejector was almost (80%) oxygen saturated, despite a very low residence time in the hydro-ejector (<50 ms).

Conversely, the aero-ejector is gas driven. Its internal geometry (see Fig. 1) induces a gas flow contraction producing a depression inside the aero-ejector which naturally drags the liquid along. However, this liquid flow rate is in this case very low and a liquid pump must then be used to adjust the desired liquid flow rate into the aero-ejector. Inside, liquid is dispersed into tiny drops by perturbations created by an internal constriction. This two-phase flow is then injected into the gas–liquid separation column where the gas is now dispersed into bubbles over a large size range. The two-phase flow in the separation column is very turbulent and mass transfer is still effective.

Unlike Venturi type contactors, the aero-ejector induces a significant pressure drop: the flow structure is similar to that obtained when a diaphragm is placed in a pipe. The energy consumption is thus greater than in a Venturi but this structure generates high turbulence inside the aero-ejector and in the separation column. This is favourable to an increase in both gas–liquid interfacial area and mass transfer coefficient.

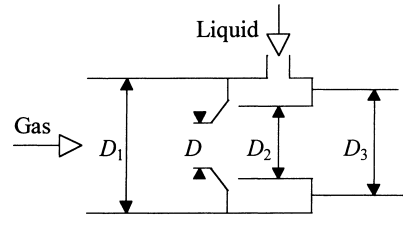

Fig. 1. The principle of the aero-ejector.

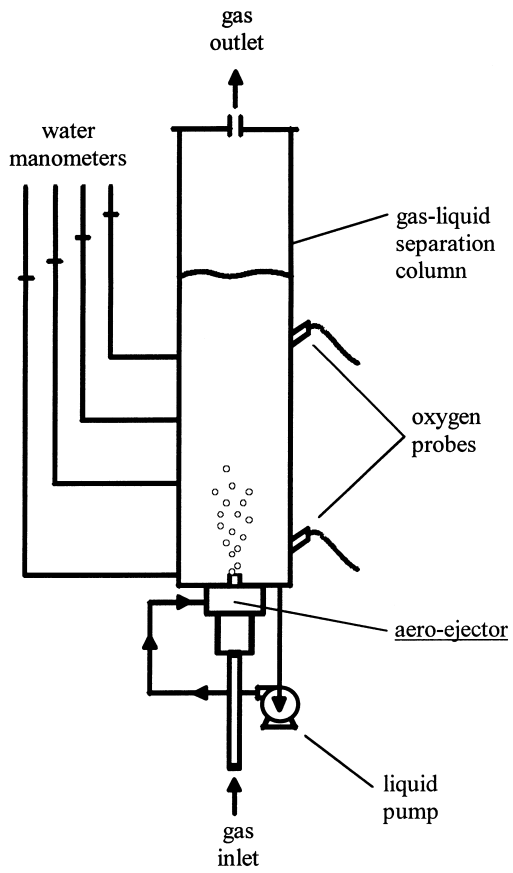

Fig. 2. Experimental set-up for oxygen absorption study.

3. Materials and methods

The variation in the inner diameter in the aero-ejector is the basis of its operating principle (see Fig. 1): creation of a *vena contracta* and generation of turbulence by the high gas acceleration. The aero-ejector studied here has the following dimensions: $D = 4 \times 10^{-3}$ m, $D_1 = 32 \times 10^{-3}$ m, $D_2 = 6.3 \times 10^{-3}$ m and $D_3 = 10.6 \times 10^{-3}$ m. The gas–liquid contacting system where it is implemented is presented in Fig. 2. The phase separation column (internal diameter: 0.153 m) contains a given liquid volume V_L, between 4.6×10^{-3} and 23×10^{-3} m^3. The external volume in the liquid recirculation loop has been evaluated at 2.36×10^{-3} m^3.

Gas was fed to the system by the laboratory compressed-air network. A pressure regulator and a needle valve fitted upstream of the system gas input were used to adjust gas flow rate. Liquid in the phase separation column was recirculated through the aero-ejector by a centrifugal pump (Flygt, France, PRX 60 Model).

Pressures were measured with fast pressure sensors (Validyne, USA) and flow rates with calibrated rotameters (Krohne, France). Gas flow rates were systematically referred to 20°C and 101 325 Pa (1 atm). Gas hold-up was measured by a manometric method using four water manometers at different heights in the phase separation column (0.25, 0.50, 0.75 and 1.00 m from the bottom). Table 1 shows the ranges of variation in the studied parameters. Operating conditions were deduced from a potential industrial application and were : $Q_G = 694 \times 10^{-6}$ m^3 s^{-1}, $Q_L = 20.8 \times 10^{-6}$ m^3 s^{-1} with $\Delta P = 0.2 \times 10^5$ Pa, the gas phase pressure drop, imposed by the industrial use of blowers or fans for gas compression.

For the oxygen transfer study (set up in Fig. 2) oxygen concentration in the liquid was measured with fast oxygen probes (Electrosense, UK). Their time constants (i.e., time needed to attain 63% oxygen saturation signal after an oxygen partial pressure input step) were experimentally determined in our laboratory and were comprised between 0.4 s for a step in gaseous atmosphere and 0.8 s for a sudden probe transfer from N_2 to O_2 saturated water. Two oxygen probes were used to verify the assumption of perfectly mixed liquid phase. One was placed at the bottom of the separating column and the other 0.05 m under the liquid free surface.

The same experimental set-up was used for the ethanol mass transfer study. Gaseous ethanol concentration was so low ($\cong 5 \times 10^{-3}$ kg m^{-3}) that its measurement was not possible and only liquid measurements were done by gas chromatography. Air–ethanol gas mixtures of known concentration at given temperature were generated by a specific system described in Fig. 3. A peristaltic pump was used to bring liquid ethanol (analytical quality, ethanol concentration = 753.78 kg m^{-3}) through a water cooled heat exchanger from its reservoir to the vaporizer (160 W, 100°C). The role of the heat exchanger is to avoid ethanol inflammation in the reservoir. To prevent condensation after the vaporizer, the gaseous ethanol was mixed with pre-heated air (100°C). This pre-heating was carried out in another heat exchanger with steam as the heating fluid. The gas mixture was then cooled to working temperature in a third exchanger. In this last device, the use of air as the cooling fluid has been proved to be more convenient and more accurate than water for the gas mixture temperature regulation. The ethanol concentration in the gas phase at aero-ejector input, C_{Gin}, is calculated as the ratio of the ethanol mass flow rate (computed from ethanol reservoir weighing) to the gas flow rate, Q_G. The gas

Table 1
Ranges of variation of the studied parameters

Gas flow rate (10^{-6} m^3 s^{-1})	Liquid flow rate (10^{-6} m^3 s^{-1})	Height of liquid in separation column (m)	Liquid volume in separation column (m^3)	Pressure drop (10^5 Pa)
300–2000	0–70	0–1.25	0–0.023	0–0.700

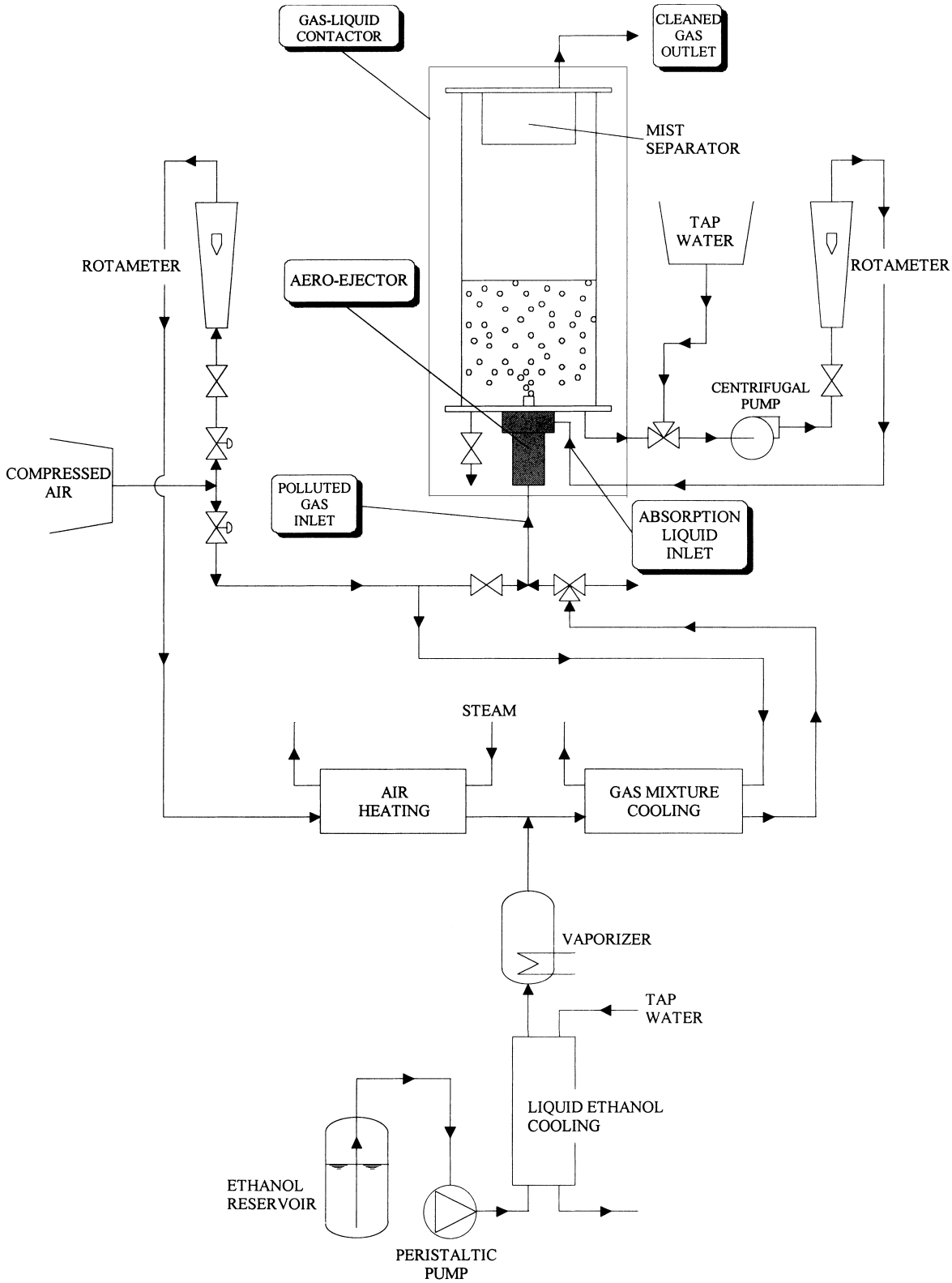

Fig. 3. Experimental set-up for ethanol absorption study.

and liquid temperatures, regulated by heat exchangers to $\pm 0.5^{\circ}C$, determine the gas–liquid interface temperature and hence the Henry constant, He. 10 ml samples were taken at the bottom of the separation column in test tubes. These latter were hermetically closed with plastic caps and immediately placed in melting ice to prevent ethanol evaporation. An internal standard (2-propanol) method was used to measure the ethanol concentration in the gas chromatograph

(Hewlett-Packard 5700A) equipped with a packed column (length: 1.5 m, diameter: 0.002 m) and a flame ionization detector. The stationary phase was Porapak Q® (Water Associates Inc.). Hydrogen, nitrogen and air flow rates were 30, 30 and 240 ml min^{-1} respectively. The injector, oven and detector temperatures were respectively, 300°C, 170°C and 300°C.

4. Results and discussion

4.1. Hydrodynamic characteristic

The pressure drop of the aero-ejector is an essential characteristic for its scale-up. Rotary blowers used in industry cannot generally give pressures higher than 0.25×10^5 Pa. The experimental results for the laboratory scaled contactor plotted on Fig. 4 have been analysed by de Billerbeck and Fonade [18]. The following correlation was obtained:

$$\Delta P_G = \left(7.13 \times 10^9 + 1.30 \times 10^{11} \times \frac{Q_L}{Q_G}\right) Q_G^2 + 4.41 \times 10^{12} \times Q_L^2 \quad (1)$$

This correlation is composed of three terms: the pressure drop due to the abrupt spreading of the gas flow downstream of the *vena contracta* (term in Q_G^2); the increase of the downstream pressure due to the liquid flow (term in Q_L^2) and the mutual influence of the gas and liquid phases inside the two-phase flow (term in Q_L/Q_G).

4.2. Absorption from air into water of a slightly soluble gas, oxygen

Considering the low solubility of oxygen in water (high value of the Henry constant, He), the oxygen volumetric overall mass transfer coefficient K_La is practically equal to the oxygen volumetric liquid-film mass transfer coefficient k_La. This oxygen volumetric mass transfer coefficient, k_La, was determined by the conventional dynamic method: gassing-out with nitrogen and then oxygenation with air [19]. The oxygen probe time constant (0.4–0.8 s) has not been taken into account in k_La determination since it is small enough compared to $1/k_La$ (9–80 s) to avoid any signal deformation by the probe response. Moreover, the liquid volume V_L in the gas–liquid separation column is 18.4×10^{-3} m^3 whereas the liquid recirculating loop volume is 2.36×10^{-3} m^3. This loop should thus not influence the k_La measurement since it is small compared to the total liquid volume (20.76×10^{-3} m^3). From the hypothesis that the oxygen composition in the air is not significantly modified by the oxygen transfer to the liquid phase (low solubility) and that the liquid phase is perfectly mixed, the mass transfer balance is then given by Eq. (2):

$$\frac{dC_L}{dt} = k_La\left(C_L^* - C_L\right) \quad (2)$$

where C_L is the instantaneous oxygen concentration in the liquid phase (water) and C_L^* is the liquid oxygen concentration in equilibrium with the gas phase (air). When k_La is considered to be independent of time, integration of Eq. (2) with $C_L = 0$ at $t = 0$ gives

$$C_L(t) = C_L^*\left(1 - e^{-k_La t}\right) \quad (3)$$

The oxygen volumetric liquid-film mass transfer coefficient k_La was determined by fitting Eq. (3) to experimental values of $C_L(t)$.

Fig. 5 shows the measured oxygen volumetric liquid-film mass transfer coefficients for different gas and liquid flow rates. These results were obtained with the experimental set-up illustrated in Fig. 2, the liquid height in the gas–liquid separation column being 1.0 m (total liquid volume = 20.76×10^{-3} m^3, recirculation loop

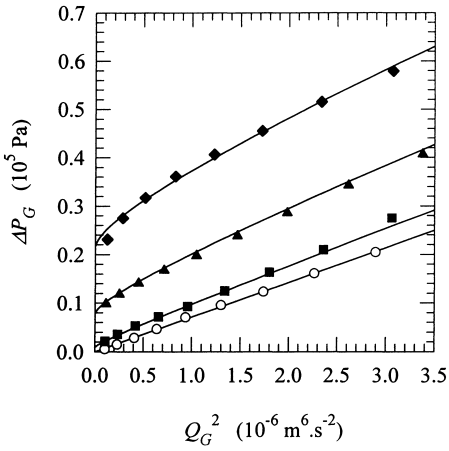

Fig. 4. Hydrodynamic behaviour of the aero-ejector: gas pressure drop ΔP_G vs. gas and liquid flow rate. Q_L (10^{-6} m^3 s^{-1}) = ○ 0, ■ 13.89, ▲ 41.67, ◆ 69.44.

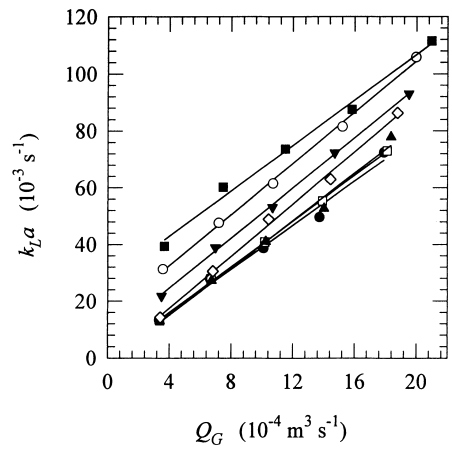

Fig. 5. Oxygen volumetric liquid-film mass transfer coefficient k_La vs. gas and liquid flow rate. Q_L (10^{-6} m^3 s^{-1}) = ● 0, □ 6.94, ▲ 13.89, ◇ 27.78, ▼ 41.67, ○ 55.56, ■ 69.44.

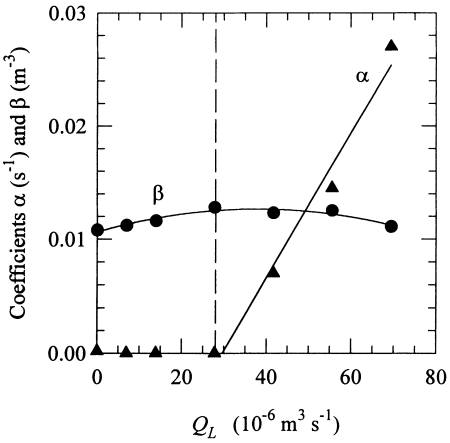

Fig. 6. Variation of coefficients α and β as a function of Q_L (Eq. (4)).

volume $= 2.36 \times 10^{-3}$ m^3). Fig. 5 shows a series of parallel lines showing that the gas flow rate influence on the mass transfer coefficient k_La for a given liquid flow rate may be represented by a linear equation :

$$k_La = \alpha + \beta Q_G \tag{4}$$

Values of α and β are given in Fig. 6. We can see that coefficient β, the slope of the curve, varies only slightly with the liquid flow rate and has a quasi constant value of $(12 \pm 1) \times 10^{-3}$ m^3. On the other hand, coefficient α is zero for liquid flow rates lower than 30×10^{-6} m^3 s^{-1} and then increases linearly for liquid flow rate values up to 70×10^{-6} m^3 s^{-1}. Increasing the liquid flow rate corresponds to a greater injection of momentum into the gas–liquid separation column. The column being an almost closed volume, a faster circulation structure is obtained and consequently the local velocities of the descending liquid are higher. Hence, gas bubbles are slowed down along their ascending path and gas retention time is increased. This enhances the mass transfer coefficient k_La by increasing particularly the specific interfacial area a. The threshold value of 30×10^{-6} m^3 s^{-1} could be considered as the minimum liquid flow in the aero-ejector itself to produce significant mass transfer compared to mass transfer in the separation column.

The power input necessary for a given mass transfer performance is an essential characteristic of a gas–liquid contactor. In the contactor studied here, power is introduced in two forms : the power necessary for gas compression to overcome the pressure drop of the whole system, W_G, and the hydraulic power W_L necessary for recirculating the liquid through the aero-ejector. The latter is much smaller.

The power for gas compression may be calculated from the equation of an isentropic transformation:

$$W_G = P_{atm} Q_G \frac{\gamma}{\gamma - 1} \left[\left(\frac{P_{Gin}}{P_{atm}} \right)^{(\gamma-1)/\gamma} - 1 \right] \tag{5}$$

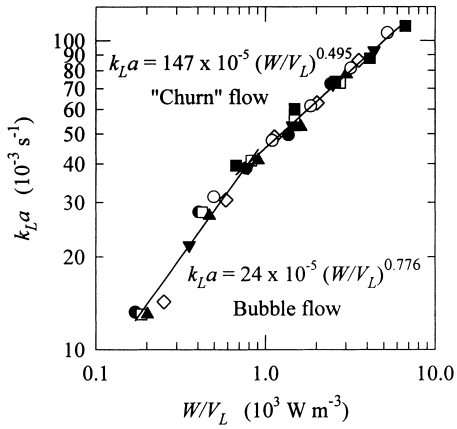

Fig. 7. Variation of the oxygen volumetric mass transfer coefficient k_La with the specific power input W/V_L. The two-phase flow regimes noted are those observed in the phase separation column. Q_L (10^{-6} m^3 s^{-1}) = ● 0, □ 6.94, ▲ 13.89, ◇ 27.78, ▼ 41.67, ○ 55.56, ■ 69.44.

The hydraulic power necessary for recirculating the liquid is given by

$$W_L = Q_L \Delta P_L \tag{6}$$

where ΔP_L is the pressure difference between the aero-ejector liquid input and its two-phase flow output. The total specific power input, W/V_L, is calculated as the total ratio of the power input to the liquid volume inside the separation column:

$$\frac{W}{V_L} = \frac{W_G + W_L}{V_L} \tag{7}$$

Fig. 7 shows the variation of the oxygen volumetric mass transfer coefficient k_La and Fig. 8 the variation of the gas hold-up, both with respect to the specific power input W/V_L. Each figure shows two distinct parts corresponding to two different gas–liquid flow regimes in the gas–liquid separa-

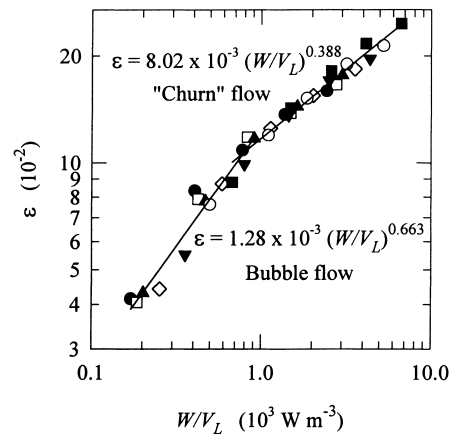

Fig. 8. Variation of the gas hold-up ε with the specific power input W/V_L. The two-phase flow regimes noted are those observed in the gas-liquid separation column. Q_L (10^{-6} m^3 s^{-1}) = ● 0, □ 6.94, ▲ 13.89, ◇ 27.78, ▼ 41.67, ○ 55.56, ■ 69.44

tion column. For $W/V_L < 0.8$ kW m^{-3}, the variation corresponds to plain bubble flow and for $0.8 < W/V_L < 7$ kW m^{-3} we visually observed a chaotic gas–liquid flow with coalescing bubbles (churn flow) that is characterized by a lower slope of the curve. The limit between these two regimes, 0.8 kW m^{-3}, corresponds to a superficial gas velocity in the separation column of 0.06 m s^{-1}. Chisti [20] observed that in bubble columns, the gas hold-up showed a change in its behaviour for the same value of the superficial gas velocity. This indicates that the gas–liquid contactor studied here, composed of an aero-ejector and of a phase separation column, behaves from a mass transfer point of view as a special bubble column and not as a gas–liquid separating system alone. But due to the aero-ejector, the energy input into this system is greater and properly used to develop mass transfer: first in the aero-ejector itself, where the power input is transformed into intense turbulence responsible for a large local mass transfer, and secondly in the phase separation column, where the turbulence produced by the two-phase jet is responsible for the particular behaviour of this bubble column.

4.3. Absorption from air into water of a very soluble gas, ethanol

The ethanol volumetric overall mass transfer coefficient, K_Ga, was determined by measuring the variation of ethanol concentration in the liquid with time.

In view of the ethanol Henry constant value, the parameter $(1/\mathrm{He})(D_L/D_G)^{1/2}$, where D_L and D_G are the ethanol liquid and gaseous phase diffusion coefficients, is much higher than 1. Under these conditions, ethanol transfer is controlled by the gas phase mass transfer resistance. This is confirmed by the linear variation in liquid phase ethanol concentration for initial time values. Hence, the volumetric mass transfer rate $K_Ga(C_G - C_G^*)$ reduces to K_GaC_G since C_G^* is negligible compared to C_G.

Considering a plug flow behaviour for the gas phase, its ethanol mass balance is given by

$$Q_G\,\mathrm{d}C_G = -K_GaC_G\Omega\,\mathrm{d}z \tag{8}$$

Assuming constant K_Ga and Q_G, integration of equation Eq. (8) gives

$$Q_G \ln\left(\frac{C_G}{C_{Gin}}\right) = -K_GaV_L \tag{9}$$

As shown by the experimental results given in Fig. 9, the ethanol concentration in the liquid as a function of time is almost a linear curve and the volumetric mass transfer rate $\mathrm{d}C_L/\mathrm{d}t = m$ is thus constant. Consequently, the liquid and gas phases overall mass balance can be calculated by

$$V_Lm = Q_G(C_{Gin} - C_G) \tag{10}$$

In this equation, the accumulation term in the gas phase balance is neglected.

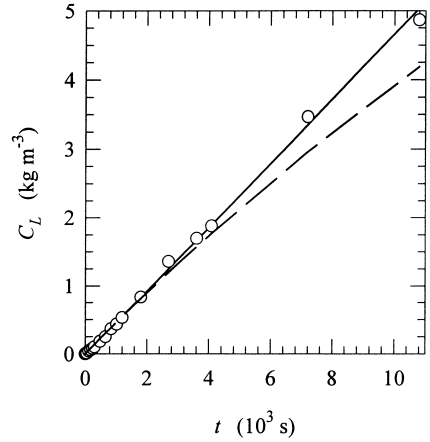

Fig. 9. Ethanol absorption. Operating condition: $T = 12.5$°C, $Q_G = 1.024 \times 10^{-3}$ m^3 s^{-1}, $Q_L = 27.78 \times 10^{-6}$ m^3 s^{-1}, $V_L = 7.88 \times 10^{-3}$ m^3, $C_{Gin} = 4.259 \times 10^{-3}$ kg m^{-3}. Fitted curve (full line) and exponential curve (dashed line, amplitude = C_L^*, time constant = $1/K_La$).

The volumetric overall mass transfer coefficient based on the gas phase is then evaluated from Eqs. (9) and (10):

$$K_Ga = -\frac{Q_G}{V_L}\ln\left(1 - \frac{mV_L}{Q_GC_{Gin}}\right) \tag{11}$$

Given the operating conditions $Q_G = 1.024 \times 10^{-3}$ m^3 s^{-1}, $V_L = 7.88 \times 10^{-3}$ m^3, $m = 4.672 \times 10^{-4}$ kg m^{-3} s^{-1} and $C_{Gin} = 4.259 \times 10^{-3}$ kg m^{-3}, we find $K_Ga = 0.242$ s^{-1}.

We can use the results of the absorption of oxygen from air into water to evaluate the ethanol liquid-film mass transfer coefficient from the value of the oxygen mass transfer coefficient. If we assume the penetration model [21] for a liquid phase, we have

$$k_L \propto D_L^{1/2} \tag{12}$$

and assuming hydrodynamic conditions, and hence the interfacial area a as nearly the same for the absorption of both components we have

$$(k_La)_{\mathrm{ethanol}} = (k_La)_{\mathrm{oxygen}}\left(\frac{D_{\mathrm{ethanol/water}}}{D_{\mathrm{oxygen/water}}}\right)^{1/2} \tag{13}$$

The oxygen volumetric liquid-film mass transfer coefficient $(k_La)_{\mathrm{oxygen}}$ determined at 20°C under the same operating Q_G and Q_L is 0.0489 s^{-1}. Diffusivities are 0.794×10^{-9} m^2 s^{-1} for ethanol in water at 12.5°C and 2.33×10^{-9} m^2 s^{-1} for oxygen in water at 20°C [22]. Introducing these values into Eq. (13) we obtain $(k_La)_{\mathrm{ethanol}} = 0.0285$ s^{-1}.

The relative influence of liquid and gas phase resistance on mass transfer rate can be analysed from Eq. (14):

$$\frac{1}{K_Ga} = \frac{1}{k_Ga} + \frac{\mathrm{He}}{k_La} \tag{14}$$

A comparison between the overall volumetric mass transfer resistance and the liquid-film mass transfer resistance confirms that ethanol transfer in our contactor is governed by

the gas phase:

$$\frac{1}{K_G a} = 4.132\,\text{s} \qquad \frac{\text{He}}{k_L a} = 5.130 \times 10^{-3}\,\text{s} \tag{15}$$

The determinant factor controlling mass transfer is the component solubility ($\text{He} = 1.462 \times 10^{-4}$), which varies with pressure and temperature. Changes of k_L or k_G due to variation in the flow regime or of the molecular diffusivity have therefore relatively reduced effects.

The fact that ethanol concentration in the liquid phase varies linearly with time can be explained by the reduction in the mean bubble diameter with the increase of the ethanol concentration in the liquid which changes its coalescence characteristics (superficial tension, viscosity). This phenomenon is optically observable and increases the gas–liquid interfacial area and hence the ethanol transfer rate. The ethanol overall volumetric mass transfer coefficient $K_G a$ determination is nevertheless correct, since it is realized at low time values for which $K_G a$ is constant.

Extrapolation of these results to an open system for the liquid phase requires knowledge of liquid and gas phase volumetric flows, liquid and gas volumes inside the contactor and liquid phase ethanol consumption kinetics.

5. Conclusions

This work has given the first insight into the mass transfer performances of a new contacting apparatus, the aero-ejector, which allows the processing of high gas–liquid ratios in a small size device. Conventional liquid-side controlled oxygen transfer was tested which allows the quantitative comparison of this technology with existing technology. We have inserted this performance in a general comparative table (Table 2) given in the work of Charpentier [23]. We have also demonstrated the ability of this device to solve an actual engineering problem, i.e., the elimination of VOCs, assimilated here to ethanol. This technology has been implemented in a real industrial operation which was sized to process 10 000 $m^3\,h^{-1}$ of gas where it proved to be successful.

Table 2
Mass transfer performance of the aero-ejector compared to conventional gas–liquid contactors [23]

Type of reactor	$ß$ (% gas–liquid volume)	$k_L a$ ($10^{-2}\,s^{-1}$)
Countercurrent packed column	2–25	0.04–7.0
Cocurrent packed column	2–95	0.04–102.0
Bubble cap plate column	10–95	1.00–20.0
Sieve plate column	10–95	1.00–40.0
Bubble column	60–98	0.50–24.0
Packed bubble column	60–98	0.50–12.0
Horizontal and coiled tube reactor	5–95	0.50–70.0
Vertical tube reactor	5–95	2.00–100.0
Spray column	2–20	0.07–1.5
Mechanical agitated bubble reactor	20–95	0.30–80.0
Submerged and plunging jet	94–99	0.03–0.60
Hydrocyclone	70–93	2.00–15.0
Ejector reactor	–	–
Venturi	5–30	8.00–25.0
Aero-ejector (our work)	5–30	1.00–12.0

6. Nomenclature

Roman symbols

C_G	concentration in the gas, kg m^{-3}
C_{Gin}	input concentration in the gas, kg m^{-3}
C_G^*	output concentration in the gas in equilibrium with C_L, kg m^{-3}
C_L	concentration in the liquid, kg m^{-3}
C_L^*	input concentration in the liquid in equilibrium with C_G, kg m^{-3}
D	characteristic orifice diameter of the aero-ejector, m
D_1	section 1 diameter of the aero-ejector, m
D_2	section 2 diameter of the aero-ejector, m
D_3	section 3 diameter of the aero-ejector, m
D_G	gas diffusion coefficient, $m^2\,s^{-1}$
D_L	liquid diffusion coefficient, $m^2\,s^{-1}$
He	Henry's law constant, (kg m^{-3})/(kg m^{-3})
k_G	gas-film mass transfer coefficient, m s^{-1}
$k_G a$	volumetric gas-film mass transfer coefficient, s^{-1}
$K_G a$	volumetric overall mass transfer coefficient referred to gas phase, s^{-1}
k_L	liquid-film mass transfer coefficient, m s^{-1}
$k_L a$	volumetric liquid-film mass transfer coefficient, s^{-1}
m	ethanol transfer rate ($m = dC_L/dt$), kg $m^{-3}\,s^{-1}$
ΔP_L	liquid pressure drop, Pa
ΔP_G	gas pressure drop, Pa
Q_G	gas flow rate, $m^3\,s^{-1}$
Q_L	liquid flow rate, $m^3\,s^{-1}$
t	time, s
V_L	liquid volume in the gas–liquid separation column, m^3
W_G	gas compression power, W
W_L	liquid pumping power, W
W/V_L	specific power (power per liquid volume), W m^{-3}
dz	contactor differential height, m

Greek symbols

α	coefficient in Eq. (4), s^{-1}
$ß$	coefficient in Eq. (4), m^{-3}
ε	gas hold-up
Ω	contactor cross section, m^2

References

[1] C. Labit, J.M. Lebault, A. Zoulalian, Hydrodynamique des contacteurs gaz-liquide du type Venturi à émulsion fonctionnant en autoaspiration, Can. J. Chem. Eng. 64(8) (1986) 663–666.

[2] S. Touré, Contribution à l'étude de l'hydrodynamique et du transfert de matière dans les réacteurs gaz–liquide de type Venturi à émulsion, Conservatoire des Arts et Métiers de Paris, France, 1984.
[3] M. Bouhelassa, A. Zoulalian, Hydrodynamique et transfert gaz–liquide dans un bioréacteur du type 'Emulsair' fonctionnant en autoaspiration, Entropie 188/189 (1995) 39–45.
[4] M. Bouhelassa, A. Zoulalian, Hydrodynamique et transfert gaz–liquide dans un bioréacteur du type 'Emulsair' fonctionnant en autoaspiration, Entropie 188/189 (1995) 47–53.
[5] C.L. Briens, L.X. Huynh, J.F. Large, A. Castros, J.R. Bernard, M.A. Bergougnou, Hydrodynamic and gas–liquid mass transfer in downward Venturi-bubble column combination, Chem. Eng. Sci. 47 (13/14) (1992) 3549–3556.
[6] D. Hadjidakis, Etude du transfert de matière et des dépenses énergétiques dans deux laveurs gaz–liquide: le Venturi de haute énergie et l'éjecteur Venturi, Ph.D. Thesis, Institut National Polytechnique de Lorraine, Nancy, France, 1983.
[7] S.M. Belhaj, P. Guerin, N. Limnios, A. Zoulalian, G. Besson, Analyse énergétique de l'efficacité d'un absorbeur réactionnel du type Venturi à jet, Chem. Eng. J. 26 (1983) 21–32.
[8] L. Melbourne, M.L. Jackson, Aeration in Bernoulli types of devices, AIChe J. 10(6) (1964) 836–842.
[9] W.G. Bauer, A.G. Fredickson, H.M. Tsuchiya, Mass transfer characteristics of a Venturi liquid–gas contactor, Ind. Eng. Chem. Proc. Des. Dev. 2(3) (1963) 178–187.
[10] B. Rainer, C. Fonade, A. Moser, Hydrodynamics of a new type of ejector, Bioproc. Eng. 13 (1995) 97–103.
[11] N. Kholi, M. Benachour, A. Zoulalian, Mise au point d'un absorbeur par voie semi-sèche à base d'un Venturi haute énergie, Can. J. Chem. Eng. 72(2) (1994) 304–313.
[12] B.J. Azzopardi, Liquid distribution in Venturi scrubbers: the importance of liquid films on the channel walls, Chem. Eng. Sci. 48(15) (1993) 2807–2813.
[13] M. Benachour, Conception et étude d'un absorbeur à base d'un Venturi à haute énergie en vue du traitement de gaz acides par voie semi-sèche, Ph.D. Thesis, Institut National Polytechnique de Lorraine, Nancy, France, 1989.
[14] P.D. Virkar, M.M. Sharma, Mass transfer in Venturi scrubbers, Can. J. Chem. Eng. 53 (1975) 512–516.
[15] E. Haller, E. Muschelknautz, T. Schultz, Venturi scrubber calculation and optimization, Chem. Eng. Technol. 12 (1989) 188–195.
[16] R.L. Miller, D.M. Jain, M.P. Sharma, Modeling Venturi scrubber performance for particulate collection and pressure drop, Chem. Eng. Comm. 89 (1990) 101–112.
[17] R.H. Boll, Particle collection and pressure drop in Venturi scrubbers, Ind. Eng. Chem. Fund. 12(1) (1973) 40–50.
[18] G.M. de Billerbeck, C. Fonade, Characterization of a new gas–liquid contactor for the biological treatment of gaseous industrial effluents, Biotechnol. Tech. 10(10) (1996) 755–760.
[19] V. Linek, V. Vacek, P. Benes, A critical review and experimental verification of the correct use of the dynamic method for the determination of oxygen transfer in aerated agitated vessels to water, electrolyte solutions and viscous fluids, Chem. Eng. J. 34 (1987) 11–34.
[20] M.Y. Chisti, Airlift Bioreactors, Elsevier Applied Sciences, London, 1989.
[21] R. Higbie, The rate of absorption of a pure gas into a still liquid during periods of exposure, Trans. AIChE 31 (1935) 365–389.
[22] R.C. Reid, J.M. Prausnitz, B.E. Poling, The properties of gases and liquids, 4th ed., McGraw Hill Book Company, New York, 1987.
[23] J.C. Charpentier, Mass transfer rates in gas–liquid absorbers and reactors, in: T.B. Drew, G.R. Cokelet, J.W. Hoopes Jr., T. Vermeulen (Eds.), Advances in Chemical Engineering. vol. 11, Academic Press, New York, 1981, pp. 1–133.